

Raman Stress microscopy induced by laser-stimulated diamond's microbreakdown

© D.A. Pomazkin¹, P.A. Danilov¹, S.I. Kudryashov¹, V.P. Martovitsky¹, I.D. Matyaev², E.A. Vasilyev³

¹ Lebedev Physical Institute, Russian Academy of Sciences,
119991 Moscow, Russia

² Bauman Moscow State Technical University,
105005 Moscow, Russia

³ St. Petersburg „Mining“ University, 199106 St. Petersburg, Russia

e-mail: d.pomazkin@lebedev.ru

Received December 11, 2023

Revised January 09, 2024

Accepted January 16, 2024

Induced stresses caused by laser optical breakdown in natural diamond bulk polished along the (331) plane by femtosecond (300 fs) laser pulses with various voltage have been studied. By the crossed polarizing filters, the zones of compression and tension of the affected area are visualized. Stress profiles were obtained using Raman spectroscopy, as well as dependence of the stress on the laser pulse energy at key points of the profiles. The result of profiling demonstrates that the slope in tension occurs faster than the raise in compression with increase of energy pumping.

Keywords: diamond's optical breakdown, femtosecond laser pulses, Raman spectroscopy, tension stress, compression stress.

DOI: 10.61011/EOS.2024.01.58294.2-24

Introduction

Internal stresses of the diamond crystal lattice may be nominally divided into natural, occurring during crystal growth and induced as a result of some diamond impact. Considerable feature of the latter is their locality resulting in change of the crystal lattice properties only in the affected area. According to [1], such stresses affect many parameters, including charge carrier mobility, optical and strength properties of a material. Thus, in [2], diamonds were exposed to ion bombardment with further investigation of induced stresses. Magnitude of these stresses allow the degree of crystal lattice implantation and damage. The study [3] investigated the influence of this stress on the operation of electromagnetic sensors based on diamond's NV centers. These stresses cause resonant frequency shift of NV ground state and deteriorate the spin dephasing time of NV. This phenomenon is essential, because NV is a radiation-induced defect and its formation in the crystal lattice may on its own cause additional stresses.

Current scientific and technology research use diamonds as materials for creation of radiation and charge sensors. To create charge sensor on diamond, optical laser-induced breakdown is used and followed by graphitization to form three-dimension conducting channels [4–6]. Though the studies [7,8] show the negative effect of induced stresses on sensor properties, investigation of this problem is not of high priority. In particular, the existing literature pays no attention to the investigation of dependence of induced stresses on laser pulse energy.

The study investigates induced stresses after the optical breakdown with ultra-short laser pulses with various energies inside a natural diamond. The classical stress analysis [9–13] uses the Raman scattering spectroscopy method. Diamond's Raman peak shift indicates that stresses are present. Mapping in compression and tension stress directions provided induced stress profiles and dependences of induced stresses on LPO laser pulse energy.

Experimental setup description

Figure 1 shows the experiment setup. Satsuma laser radiation (pulse duration 300 fs, wavelength 515 nm, pulse repetition rate 20 kHz) was focused inside the diamond with two facets polished along plane (331) to carry out optical breakdown using lens $NA = 0.65$, 10 \times , Levenhuk. The diamond was moved using the xyz table connected to the laptop that was also used for laser system control. Crystal-lattice orientation of the sample facets was defined by X-ray diffraction using X'PertPro MRD Extended equipment.

The experiment used a natural diamond sample (Figure 2, a) that contained inherent stresses before modification (Figure 2, b). Inside the diamond at a depth of 50 μm from the surface, a matrix was recorded that contained optical microbreakdowns spaced at 50 μm between points, laser pulse energies from 43.5 to 64.9 nJ (Figure 2, c) and exposure time 1 s in each point. The crossed polarization filters (Figure 2, c) show the stresses induced by breakdown. Image background is nonuniform due to the presence of

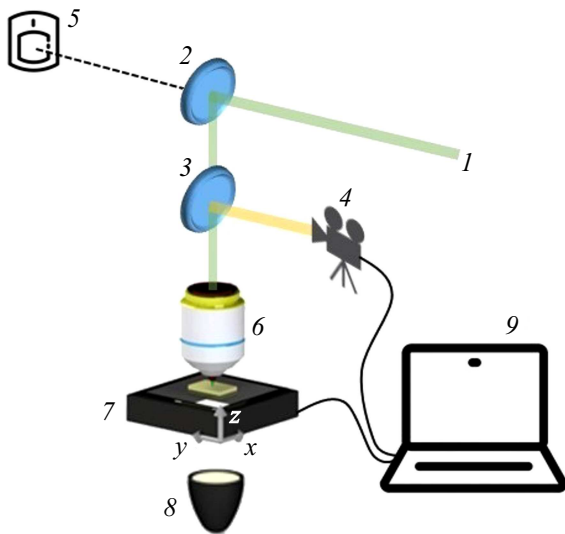


Figure 1. Experimental setup: 1 — 515 nm laser emission, 2 — folding mirror, 3 — dichroic mirror, 4 — CCD camera, 5 — OphirPD10-C energy meter, 6 — lens $NA = 0.65$, $10\times$, Levenhuk, 7 — xyz table with diamond sample, 8 — bottom backlighting, 9 — laptop for table control and laser emission supply.

inherent stresses in the diamond before laser recording. Induced stresses form a two-sheet compression (light regions) and tension (dark areas) stress pattern relative to the microbreakdown. The induced stresses were analyzed using the points located in the uniform initial background signal distribution zone [14].

The diamond sample corresponds to the IaA type based on the preliminary characterization by the infrared (IR) Fourier spectroscopy technique. absorption spectra (Figure 3) were recorded using Mikran-3 IR Fourier spectromicroscope through a $28 \times 28 \mu\text{m}$ square diaphragm.

Experimental results

The study mapped the compression and tension areas (Figure 4, *a*) by Raman line peak position (stresses were recalculated in GPa as described in [13]) using Confotec MR520 confocal microscope after laser microbreakdown. The recorded profiles along the highlighted directions are shown in Figure 4 *a*. For analysis, three key points were taken (shown by vertical dotted lines and numbers 1, 2 and 3). Point 1 corresponds to the modified zone center, point 2 corresponds to the microbreakdown region boundary, point 3 corresponds to the minimum stress region. The optical images show that the diameter of the microbreakdown region is $\sim 8 \mu\text{m}$ (highlighted by two purple vertical lines). General profile pattern is W-shaped for tension and M-shaped for compression with dips and rises, respectively. Though the profile pattern (Figure 4, *a*) is shown only for two laser pulse energies to avoid overloading of the figure, five energies were used to plot the dependences of stresses on laser pulse energy (Figure 4, *b*).

Figure 4, *b* displays the dependence of stresses on laser pulse energy along tension directions (empty triangles) and compression directions (filled triangles). Point 1 (black circles) chosen in the microbreakdown region center is in a slight tension region ($\sim -0.5 \text{ GPa}$) and is common for the profiles. Point 3 (green) is at $10 \mu\text{m}$ from the microbreakdown center and demonstrates no or minimum stresses. Point 2 (blue) is in the maximum stress region and reflects the sought-for dependence of induced stresses on the laser emission energy. Comparison of linear compression and tension approximation (dark blue dashed straight lines) suggests multiply quicker growth of tension than of compression – slope coefficient of straight line for compression is $\sim 0.011 \text{ GPa/nJ}$, and for tension is $\sim -0.053 \text{ GPa/nJ}$. Maximum stress in point 2 for tension is 1.87 GPa , and for compression is 0.89 GPa .

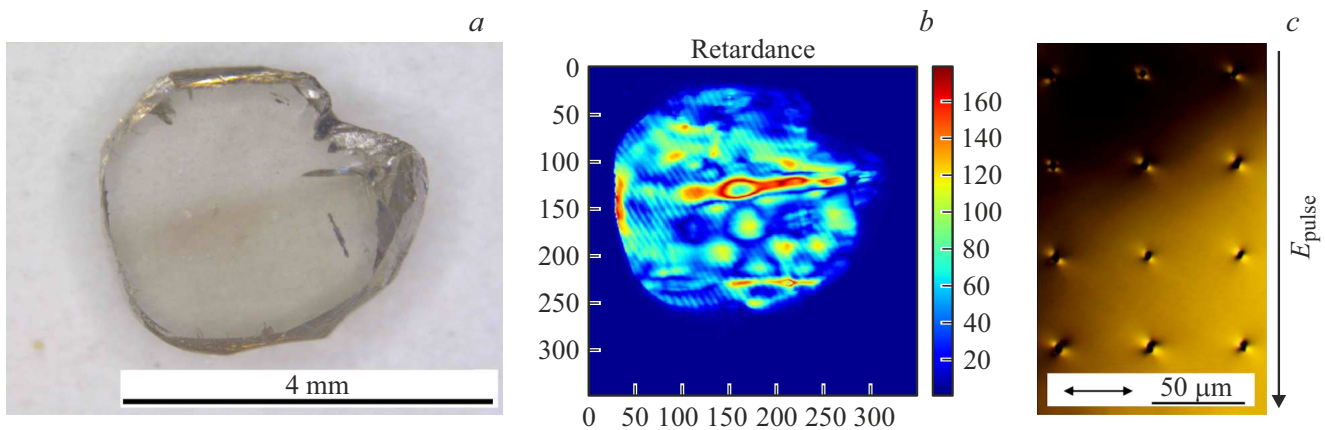


Figure 2. Diamond sample used for investigations: (a) Photograph of the sample, (b) birefringent image of the sample, (c) recorded label matrix in crossed polarization filters, arrows near the scale bar show the laser radiation polarization direction during recording.

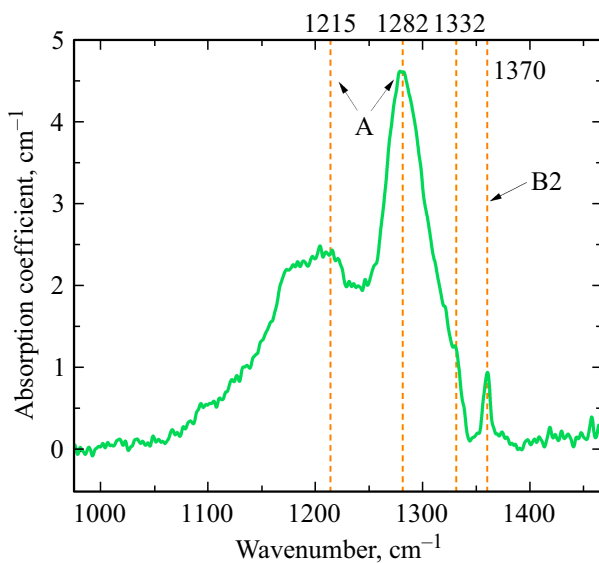


Figure 3. IR absorption spectrum of the diamond sample corresponding to the IaA type. Vertical dashed lined show the typical absorption peaks for A and B2 defects presented in the diamond sample.

Conclusion

The study investigates induced stresses that occur after optical microbreakdown of a natural diamond by femtosecond laser pulses with varied energy. The experiment has shown that after modification two-sheet tension and compression stress patterns are formed and the Raman spectroscopy method was used to analyze and profile these patterns. The recorded dependences demonstrate the

growth of tension and compression stresses with an increase in laser pulse energy. However, the slope coefficient for the linear approximation of compression stresses, as well as maximum stresses, is lower in absolute value than of tension stresses. It has been established that the induced stresses were clearly expressed in the area of the damaged zone boundary, propagated beyond the visible region of microbreakdown and decreased to zero at a distance of about $10\ \mu\text{m}$.

Funding

The study was supported by a grant provided by the Russian Science Foundation (project № 21-79-30063), <https://rscf.ru/en/project/21-79-30063/>.

Conflict of interest

The authors declare that they have no conflict of interest.

References

- [1] D.A. Broadway, B.C. Johnson, M.S.J. Barson, S.E. Lillie, N. Dontschuk, D.J. McCloskey, A. Tsai, T. Teraji, D.A. Simpson, A. Stacey, J.C. McCallum, J.E. Bradby, M.W. Doherty, L.C.L. Hollenberg, J.P. Tetienne. *Nano Lett.*, **19** (7), 4543 (2019). DOI: 10.1021/acs.nanolett.9b01402
- [2] R.A. Khmel'nitsky, V.A. Dravin, A.A. Tal, M.I. Latushko, A.A. Khomich, A.V. Khomich, A.S. Trushin, A.A. Alekseev, S.A. Terentiev. *Nucl. Instr. Meth. Phys. Res. B*, **304**, 5 (2013). DOI: 10.1016/j.nimb.2013.03.030
- [3] M.J. Turner, R. Trubko, J.M. Schloss, C.A. Hart, M. Wesson, D.R. Glenn, R.L. Walsworth. *Phys. Rev. B*, **100** (17), 174103 (2019). DOI: 10.1103/PhysRevB.100.174103

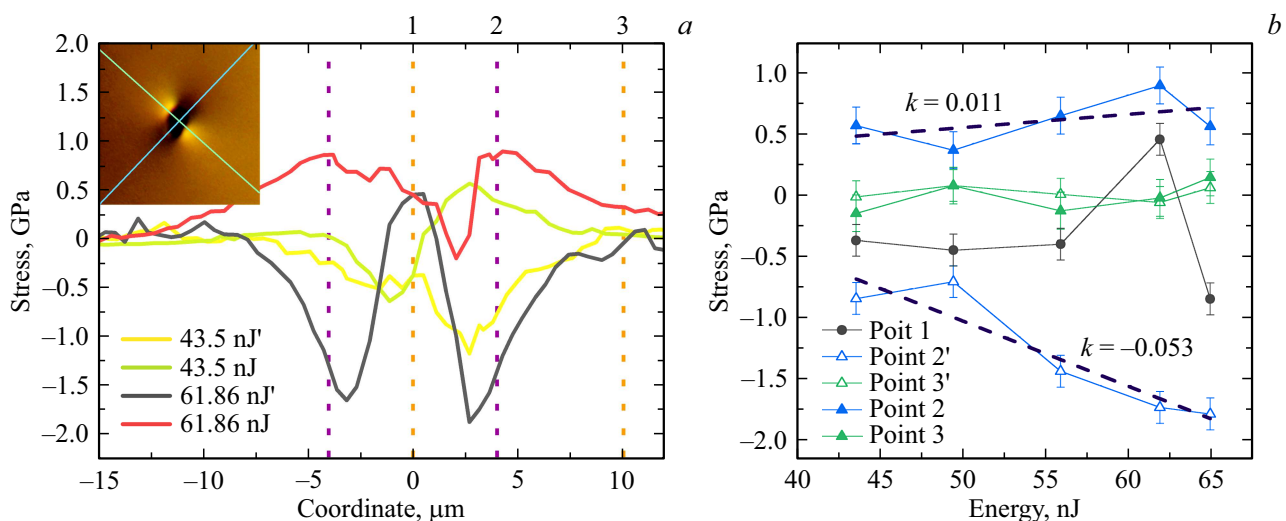


Figure 4. Investigations of induced stresses by the Raman spectroscopy technique. (a) Profiles in tension directions (laser pulse energies in the lower left-hand angle of the figure are marked by the bar) and in compression directions (without bar), microbreakdown region profiling directions are shown in the Detail: green — compression, blue — tension. (b) Dependence of induced stresses on laser pulse energy in key points: point 1 — damaged region center (black circles), points 2, 3 — damage region boundary (empty triangles — for tension and filled triangles — for compression).

- [4] A.A. Khomich, K.K. Ashikkalieva, A.P. Bolshakov, T.V. Kononenko, V.G. Ralchenko, V.I. Konov, P. Oliva, G. Conte, S. Salvatori. *Diamond and Related Materials*, **90**, 84 (2018). DOI: 10.1016/j.diamond.2018.10.006
- [5] M. Girolami, A. Bellucci, P. Calvani, S. Orlando, V. Valentini, D.M. Trucchi. *Appl. Phys. A*, **117** (1), 143 (2014). DOI: 10.1007/s00339-014-8310-x
- [6] T.V. Kononenko, E.V. Zavedeev, V.V. Kononenko, K.K. Ashikkalieva, V.I. Konov. *Appl. Phys. A*, **119** (2), 405 (2015). DOI: 10.1007/s00339-015-9109-0
- [7] S.S. Salvator, C.R. M.C. Ross, C.G. Cont, K.T. Kononenko, K.M. Komleno, K.A. Khomic, R.V. Ralchenk, K.V. Kono, P.G. Provata, J.M. Jaksi. *IEEE Sensors J.*, **19** (24), 11908 (2019). DOI: 10.1109/JSEN.2019.2939618
- [8] M.C. Rossi, S. Salvatori, G. Conte, T. Kononenko, V. Valentini. *Opt. Mater.*, **96**, 109214 (2019). DOI: 10.1016/j.optmat.2019.109214
- [9] K.H. Chen, Y.L. Lai, J.C. Lin, K.J. Song, L.C. Chen, C.Y. Huang. *Diamond and Related Materials*, **4** (4), 460 (1995). DOI: 10.1016/0925-9635(94)05319-7
- [10] E. Anastassakis. *J. Appl. Phys.*, **86** (1), 249 (1999). DOI: 10.1063/1.370723
- [11] A. C. Ferrari, J. Robertson. *Phys. Rev. B*, **61** (20), 14095 (1999). DOI: 10.1103/PhysRevB.61.14095
- [12] A.C. Ferrari, J. Robertson. *Phil. Trans. Roy. Soc. London A*, **362** (1824), 2477 (2004). DOI: 10.1098/rsta.2004.1452
- [13] H. Boppart, J.I. Silvera. *Phys. Rev. B*, **32**, 1423 (1985). DOI: 10.1103/PhysRevB.32.1423
- [14] G.K. Krasin, N.G. Stsepuro, V.P. Martovitsky, M.S. Kovalev. *Opt. i spektr.*, **130** (4), 507 (2022). (in Russian) DOI: 10.61011/EOS.2024.01.58294.2-24

Translated by E.Ilinskaya